

This is a self-archived version of an original article. This version may differ from the original in pagination and typographic details.

Author(s): Tarvainen, O.; Kalvas, T.; Koivisto, H.; Kronholm, R.; Marttinen, M.; Sakildien, M.; Toivanen, V.; Izotov, I.; Skalyga, V.; Angot, J.

Title: Plasma diagnostic tools for ECR ion sources : What can we learn from these experiments for the next generation sources

Year: 2019

Version: Published version

Copyright: © 2019 Authors

Rights: In Copyright

Rights url: <http://rightsstatements.org/page/InC/1.0/?language=en>

Please cite the original version:

Tarvainen, O., Kalvas, T., Koivisto, H., Kronholm, R., Marttinen, M., Sakildien, M., Toivanen, V., Izotov, I., Skalyga, V., & Angot, J. (2019). Plasma diagnostic tools for ECR ion sources : What can we learn from these experiments for the next generation sources. *Review of Scientific Instruments*, 90(11), Article 113321. <https://doi.org/10.1063/1.5127050>

Plasma diagnostic tools for ECR ion sources—What can we learn from these experiments for the next generation sources

Cite as: Rev. Sci. Instrum. **90**, 113321 (2019); <https://doi.org/10.1063/1.5127050>

Submitted: 08 September 2019 . Accepted: 20 October 2019 . Published Online: 22 November 2019

O. Tarvainen, T. Kalvas , H. Koivisto, R. Kronholm , M. Marttinen , M. Sakildien, V. Toivanen , I. Izotov , V. Skalyga , and J. Angot

COLLECTIONS

Paper published as part of the special topic on [Proceedings of the 18th International Conference on Ion Sources](#)



View Online



Export Citation



CrossMark

ARTICLES YOU MAY BE INTERESTED IN

[Optimization design of magnetic filter for the prototype RF negative ion source at ASIPP](#)
Review of Scientific Instruments **90**, 115117 (2019); <https://doi.org/10.1063/1.5128256>

[Study of continuous wave 33 keV H⁻ beam transport through the low energy beam transport section](#)

Review of Scientific Instruments **90**, 113323 (2019); <https://doi.org/10.1063/1.5128591>

[Extension of high power deuterium operation of negative ion based neutral beam injector in the large helical device](#)

Review of Scientific Instruments **90**, 113322 (2019); <https://doi.org/10.1063/1.5128529>

Lock-in Amplifiers
... and more, from DC to 600 MHz



Plasma diagnostic tools for ECR ion sources—What can we learn from these experiments for the next generation sources

Cite as: Rev. Sci. Instrum. 90, 113321 (2019); doi: 10.1063/1.5127050

Submitted: 8 September 2019 • Accepted: 20 October 2019 •

Published Online: 22 November 2019



O. Tarvainen,^{1,2,a)} T. Kalvas,² H. Koivisto,² R. Kronholm,² M. Marttinen,² M. Sakildien,^{2,3} V. Toivanen,² I. Izotov,⁴ V. Skalyga,⁴ and J. Angot⁵

AFFILIATIONS

¹STFC, ISIS Pulsed Spallation Neutron and Muon Facility, Rutherford Appleton Laboratory, Harwell OX11 0QX, United Kingdom

²University of Jyväskylä, 40500 Jyväskylä, Finland

³Accelerator Department, iThemba LABS (Laboratory for Accelerator Based Sciences), P.O. Box 722, Somerset West 7192, South Africa

⁴Institute of Applied Physics, RAS, 46 Ul'yanova St., 603950 Nizhny Novgorod, Russian Federation

⁵Université Grenoble-Alpes, CNRS-IN2P3, Grenoble Institute of Engineering (INP), LPSC, 38000 Grenoble, France

Note: Invited paper, published as part of the Proceedings of the 18th International Conference on Ion Sources, Lanzhou, China, September 2019.

^{a)}Electronic mail: olli.tarvainen@stfc.ac.uk

ABSTRACT

The order-of-magnitude performance leaps of ECR ion sources over the past decades result from improvements to the magnetic plasma confinement, increases in the microwave heating frequency, and techniques to stabilize the plasma at high densities. Parallel to the technical development of the ion sources themselves, significant effort has been directed into the development of their plasma diagnostic tools. We review the recent results of Electron Cyclotron Resonance Ion Source (ECRIS) plasma diagnostics highlighting a number of selected examples of plasma density, electron energy distribution, and ion confinement time measurements, obtained mostly with the second-generation sources operating at frequencies from 10 to 18 GHz. The development of minimum-B ECR ion sources based on the superposition of solenoid and sextupole fields has long relied on semiempirical scaling laws for the strength of the magnetic field with increasing plasma heating frequency. This approach is becoming increasingly difficult with the looming limits of superconducting technologies being able to satisfy the magnetic field requirements at frequencies approaching 60 GHz. Thus, we discuss alternative ECRIS concepts and proposed modifications to existing sources that are supported by the current understanding derived from the plasma diagnostics experiments.

Published under license by AIP Publishing. <https://doi.org/10.1063/1.5127050>

I. ECRIS GENERATIONS AND SCALING LAWS

The performance of Electron Cyclotron Resonance Ion Sources (ECRISs)¹ has improved dramatically over the past decades, owing to improvements of the magnetic plasma confinement, increases in the microwave heating frequency, and techniques to stabilize the plasma at high densities. The design of modern ECR ion sources is based on semiempirical scaling laws, suggesting most importantly that the extracted current at the peak of the ion charge state distribution (CSD) scales with the microwave frequency squared,² i.e.,

$$I_{peak} \propto f_{RF}^2. \quad (1)$$

The frequency scaling assumes that the strength of the minimum-B magnetic field (solenoid and sextupole) is adjusted accordingly to fulfill the scaling laws,³

$$B_{inj}/B_{ECR} = 4, \quad (2)$$

$$B_{rad}/B_{ECR} = 2, \quad (3)$$

$$B_{ext} \approx 0.9B_{rad} = 1.8B_{ECR}, \quad (4)$$

$$B_{\min} \approx 0.4B_{\text{rad}} = 0.8B_{\text{ECR}}, \quad (5)$$

where B_{inj} , B_{rad} , B_{ext} , and B_{\min} are the fields at the injection, radial wall of the plasma chamber, extraction, and B-minimum, whereas $B_{\text{ECR}}[\text{T}] = f[\text{GHz}]/28$ is the resonance field for cold ($\gamma = 1$) electrons. The scaling of the injection, extraction, and radial fields can be explained by the plasma confinement. The upper limit of B_{\min} is believed to be due to the kinetic plasma instability threshold,⁴ which is typically found⁵ at B_{\min}/B_{ECR} of 0.7–0.8. Thus, high-performance superconducting sources, such as VENUS,⁶ are typically operated with B_{\min}/B_{ECR} in the range of 0.4–0.7.

A direct comparison of different ECRIS generations is complicated as the CSD shifts toward higher charge states with increasing frequency. More importantly, the effects of the frequency and magnetic field cannot be separated as $f_{\text{RF}} \propto B$, but it is evident from the experiments that increasing the microwave frequency and the magnetic field strength improves the extracted currents of high charge state ions, implying enhanced plasma energy content $n_e k T_e$. Several explanations for the frequency scaling have been proposed. These include reaching the critical (cutoff) plasma density and so-called RF pitch angle scattering presumably limiting the electron density, both scaling with f_{RF}^2 .

The magnetic field scaling sets a practical limit for the 1st and 2nd generation (6.4–18 GHz) room-temperature (RT) ion sources based on electromagnetic coils and a permanent magnet sextupole. Thus, the 3rd generation (20–28 GHz) sources rely on superconducting technologies. Building a 4th generation ECRIS up to 56 GHz is feasible using the state-of-the-art Nb3Sn superconducting wire,⁷ whereas a further increase of the frequency and magnetic field requires either accepting a substandard field strength or research and development on innovative concepts, e.g., the ARC-ECRIS feasible up to 100 GHz,⁸ as well as improved microwave-plasma coupling structures.^{9,10} Figure 1 shows the frequency dependence of the maximum solenoid field at the injection (B_{inj}) and the sextupole field at the chamber wall (B_{rad}) together with the cut-off electron density ($\omega_{pe} = \omega_{\text{RF}}$), summarizing the challenges related to the frequency scaling.

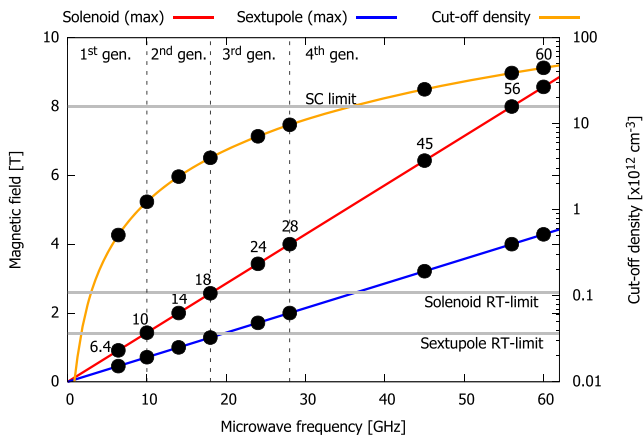


FIG. 1. Frequency scaling of the minimum-B ECRIS solenoid and sextupole magnetic fields and cut-off plasma density. The dots mark commonly applied microwave frequencies.

It has been recently proposed¹¹ that the power required to operate high frequency sources up to their full capacity should also scale as frequency squared, i.e.,

$$P_{\text{RF}} \propto f_{\text{RF}}^2, \quad (6)$$

and that operating a 4th generation ECRIS, e.g., at 60 GHz, would require up to 40 kW of microwave power, which poses a significant challenge on managing the localized heat load determined by the electron losses and limits the choice of applicable microwave generators and microwave-plasma coupling structures.

The frequency scaling of the extracted current implies that operation at higher frequencies will increase the total extracted currents, which in turn translates to higher extraction voltages V_{ext} to assure that the source and its extraction system operate in plasma density limited mode rather than space charge limited mode, i.e.,

$$V_{\text{ext}} \propto I_{\text{total}}^{2/3} \propto f_{\text{RF}}^{4/3}, \quad (7)$$

suggesting that the 4th generation sources operating at 56 GHz or above require extraction voltages of ≥ 75 kV.¹¹ Operating the ion source at adequate power and extraction voltage is important because the transverse emittance of the extracted beam scales as $\epsilon_{x,y} \propto B$ and, thus, the beam brightness is constant for different generation sources only if $I \propto f_{\text{RF}}^2$ or $I \propto B^2$. However, there is some experimental evidence¹² suggesting that, contrary to the theory, the transverse emittance decreases with increasing B_{ext} . This could be explained by the magnetic field strength affecting the spatial distribution of the ions¹³ at the extraction aperture.

II. HIGH CHARGE STATE ION PRODUCTION

The density of ions in the steady-state ECRIS plasma is described by the so-called balance equation,¹⁴

$$\begin{aligned} \frac{dn^q}{dt} = n_e n^{q-1} \langle \sigma v_e \rangle_{q-1 \rightarrow q}^{\text{ion}} - n_e n^q \langle \sigma v_e \rangle_{q \rightarrow q+1}^{\text{ion}} + n_0 n^{q+1} \langle \sigma v_i \rangle_{q+1 \rightarrow q}^{\text{ex}} \\ - n_0 n^q \langle \sigma v_i \rangle_{q \rightarrow q-1}^{\text{ex}} - \frac{n^q}{\tau^q} = 0, \end{aligned} \quad (8)$$

which describes the time-evolution of the ion densities of charge states $q = 1, 2, \dots, q_{\text{max}}$. The first and second terms describe the rates of electron impact ionization from/to lower/higher charge state that depend on the electron density and velocity, ionization cross section, and ion densities. The third and fourth terms describe the rates of charge exchange with neutrals populating/depoppingulating the charge state q from/to a higher/lower charge state that depend on the neutral density, ion densities and velocities, and charge exchange cross section. Finally, the last term describes the ion losses (including the extracted beam) that depend on the ion density and confinement time, the latter being a complex function of the ion temperature T_i and the properties of the electrostatic ion confinement. This is because the ions are trapped in a potential dip $\Delta\Phi$, caused by the accumulation of magnetically confined (hot) electrons to the core plasma and different loss rates of electrons and ions, resulting in an ambipolar potential barrier restricting the ion losses.¹⁵ The CSD of the ions in the ECRIS plasma is described by the set of coupled balance equations describing the densities of each charge state.

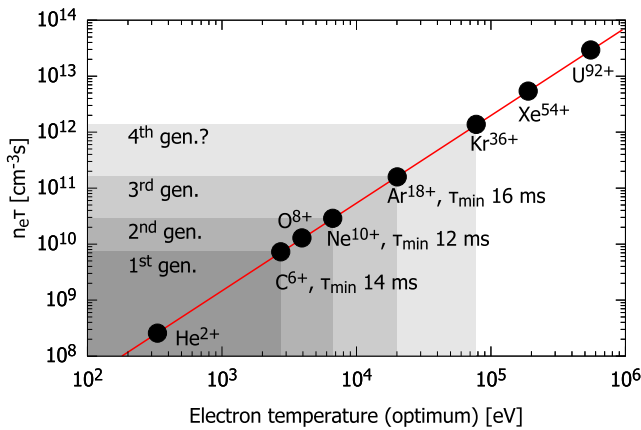


FIG. 2. The required product of $n_e\tau$ at the optimum electron temperature to produce various fully stripped ions. The minimum ion confinement times of fully stripped C, Ne, and Ar ions displayed here correspond to the optimum electron temperature and critical density at 6.4, 14, and 28 GHz, representing the limits of the 1st–3rd generation sources. The data for the so-called Golovanivsky plot are taken from Ref. 1.

In the balance equation, the extraction of ion beams is seen as a favorable loss process, which is somewhat misleading as it implies that minimizing the ion confinement time leads to higher extracted current. This is not true as the cumulative confinement time of the ions must be long enough for them to reach high charge states in the first place, and only then can the extracted currents be optimized by minimizing the confinement time, which implies that optimizing the ECRIS parameters for the production of a certain charge state is inevitably a compromise between ion confinement and escaping ion flux. Figure 2 illustrates the requirements for fully stripped ion production in terms of $n_e\tau$ and electron temperature T_e (assuming a Maxwellian electron population). The highlighted regions are covered by different ECRIS generations as deduced from experimental observations. The minimal confinement times shown for C^{6+} , Ne^{10+} , and Ar^{18+} have been calculated assuming an optimum electron temperature and cut-off electron density at 6.4, 14, and 28 GHz, i.e., the true confinement times of the fully stripped ions can be expected to be longer.

Equation (8) and Fig. 2 entail that the purpose of ECRIS plasma diagnostics should be to probe the electron density, electron energy distribution (EED), and discharge properties affecting the ion confinement time, i.e., ion temperature, plasma potential, and relative importance of each electron loss mechanism (Coulomb collisions, RF-induced pitch angle scattering, and instabilities).

III. ECRIS PLASMA DIAGNOSTICS

ECRIS plasmas can be studied reliably only by measuring plasma emission signals (radiation or particle fluxes) or the plasma response to external probe signals (injection of radiation or particle beams) as invasive diagnostic methods such as Langmuir-probes inherently affect the discharge properties (EED and CSD). Moreover, it is important to conduct all diagnostics experiments under conditions relevant for the ion source operation since seemingly

irrelevant factors, e.g., switching off the high voltage of the ion source, can change the diagnostics results dramatically¹⁶ by affecting the EED and the neutral particle density. Girard¹⁷ has published a comprehensive review of ECRIS plasma diagnostics methods and results dating back to the early 1990s and, thus, we focus on recent achievements in this field, listing only some selected examples, referring the reader to original research papers. A summarizing table (Table I) listing different plasma diagnostics techniques applicable to ECRIS plasmas is presented at the end of this section.

A. Electron density (n_e)

Measuring the electron density in ECRIS plasmas is notoriously difficult. Langmuir-probes and optical emission spectroscopy (OES), which are applicable for high-density microwave discharges dominated by 1+ ions, are not suitable for the highly charged plasmas of minimum-B ECRIS either due to their invasive nature or the pressure broadening of ion emission lines being negligible in comparison with Doppler and instrumental broadening.¹⁸ In the vacuum ultraviolet (VUV)-range, the measurement of the intensity ratios of singlet and triplet transitions of Be-like ions can yield information

TABLE I. ECRIS plasma parameters and suitable diagnostics. Most of the methods are indirect and require simultaneous use of different diagnostics tools or knowledge about another plasma parameter as discussed in this paper. Technical details about each diagnostic tool can be found in the original research papers.

| | |
|--|---|
| Electron density | Interferometry 1+ beam injection Plasma diamagnetism |
| Ion density and CSD | Optical emission spectroscopy (relative intensities) M/Q -analysis of the extracted beam Characteristic x-ray energy |
| Electron energy distribution | Wall bremsstrahlung Plasma bremsstrahlung Escaping electron spectroscopy Electron cyclotron emission Plasma diamagnetism Optical emission spectroscopy (line-ratio method) |
| Ion confinement time | Pulsed material injection (sputtering, 1+ inj. and beam current transient) |
| Ion temperature | Optical emission spectroscopy (Doppler broadening) |
| Ion collision frequency Plasma potential Instabilities | 1+ beam injection Retarding field analyzer Microwave emission Bremsstrahlung bursts Electron and ion bursts (end-loss analyzer or the extracted beam) |

on the electron density²¹ of the cold electron population assuming that the excitation and de-excitation (spontaneous vs electron impact de-excitation of metastable states) are well-understood.

Microwave interferometry, which is based on detecting the phase shift of a probe microwave beam, has been successfully applied¹⁹ to measure the average electron density in a 3.75 GHz single-solenoid ECR discharge, yielding values on the order of 10^{13} cm^{-3} , i.e., well above the critical density similar to high frequency gasdynamic ECR ion sources.²⁰ In a minimum-B ECRIS, interferometry is complicated by the low ratio of the plasma chamber dimension (line-of-sight length) to the microwave beam wavelength as well as mechanical constraints prohibiting access for the microwave launching system and receiver. Interferometry results obtained with high-frequency (18 GHz Quadrumafios) ECRIS yield values of $2\text{--}5 \times 10^{11} \text{ cm}^{-3}$, i.e., well below the critical density.²¹ VUV-diagnostics of the same source imply that the cold electron population accounts for 20%–50% of the total electron density.²¹

Measurement of the captured fraction of the incident 1+ ion beam injected into charge breeder ECRIS allows estimating the lower limit of the electron density in the minimum-B discharge.²² The 1+ probe technique has been applied on the 14.5 GHz PHOENIX charge breeder ECRIS operating at microwave power below 500 W, yielding n_e values in the range of $2\text{--}5 \times 10^{11} \text{ cm}^{-3}$, which matches the range reported for a conventional ECRIS.²¹ It is assumed that the capture of the injected 1+ ions occurs through ion-ion collisions whose frequency depends on T_i and, hence, the accuracy of the plasma density estimate could be improved by measuring T_i in the charge breeder plasma using OES to detect the Doppler broadening of the ion emission lines.¹⁸ The estimated density being on the order of 10^{11} cm^{-3} can be used to estimate the minimum ion confinement time using Fig. 2 together with the measured performance of the given charge breeder ECRIS producing fully stripped oxygen ions (or equivalent charge states of Cs). The derived cumulative ion confinement time is on the order of 10–100 ms, which matches well with the time scale of the high charge state ion beam decay transient observed with pulsed 1+ injection.²³

The plasma density and its parametric variation could also be derived from diamagnetic loop measurements²⁴ detecting the change in the plasma energy content ($n_e k T_e$) in the pulsed operation of the ECRIS if the EED and its temporal change were simultaneously measured. Unfortunately, none of the techniques described above can be used for detecting the spatial variation of the electron density, which is a severe limitation as the difference in electron and ion densities between the plasma core and peripheral region is believed to be significant as reaffirmed by particle-in-cell simulations.²⁵

B. Electron energy distribution (EED)

Information about the EED in ECRIS plasmas can be acquired indirectly by measuring the plasma and/or wall bremsstrahlung or directly by measuring the energy distribution of the electrons escaping the confinement.

Almost the whole range of photon energies of the plasma and/or wall bremsstrahlung spanning from a few kilo-electronvolts to mega-electronvolts can be measured with NaI, CdTe, or Ge x-ray detectors, whereas a Si-detector is better suited for the

measurement of characteristic x-rays.^{26–28} These detectors do not yield the spatial information of the emitted radiation contrary to CCD-based x-ray pinhole cameras.²⁹ Bremsstrahlung data can also be acquired in pulsed operation, allowing us to study how fast the plasma energy content builds up and how fast electrons are being lost from the confinement.²⁷ Time-resolved measurements also help detecting onsets of kinetic instabilities for which the best tool is a current-mode scintillator detector measuring the integrated x-ray power flux.⁴

Experiments³⁰ with the VENUS ion source at LBNL have revealed that the spectral temperature of axial plasma bremsstrahlung spectrum appears to be dependent solely on the minimum magnetic field B_{min} rather than B_{min}/B_{ECR} or the microwave frequency f_{RF} in the stable operation regime. At the same time, it was confirmed with 14, 18, and 28 GHz frequencies that the plasma energy content and maximum electron energy indeed increase with the frequency at a fixed magnetic field. Experiments in pulsed operation mode with the first and second generation sources indicate that the saturation time of the bremsstrahlung flux and spectrum is on the order of 10–100 ms, which matches well with the diamagnetic loop data and measured ion confinement times.^{27,31} Finally, recent experiments²⁸ with two 14 GHz ion sources measuring the (absolute) volumetric rate of characteristic x-ray emission allow us to deduce parametric dependencies of the inner shell ionization rate, which is directly proportional to the production rate of high charge state ions, indicating only a weak dependence on B_{min} . It is therefore concluded that the magnetic field mostly affects the hot electron population contributing to bremsstrahlung emission and ion confinement but having only a weak effect on the high charge state ion production. Furthermore, precise measurement of the characteristic x-ray emission energies that depend on the charge state of the emitting ion allows quantifying the CSD in the core plasma and comparing it to the extracted one.³²

The main challenge related to bremsstrahlung diagnostics is the ambiguous relation between the bremsstrahlung spectrum and the EED. The EED of the axially escaping electrons was measured with the JYFL 14 GHz ECRIS using the bending magnet as a spectrometer.^{33,34} It was discovered that the EED is non-Maxwellian and depends strongly on the magnetic field together with the absolute electron loss rate in the stable operation regime. These experiments³⁴ have (i) yielded direct evidence on RF-induced pitch angle scattering causing electron losses, (ii) enabled measuring the EED of the electrons expelled by kinetic instabilities, and (iii) allowed detecting the change in the EED when the kinetic instabilities limiting ECRIS performances, and being the most likely cause for the $B_{min} = 0.8B_{ECR}$ -scaling,⁵ are suppressed using double frequency heating.³⁵ The apparent limitation of the technique is that it measures the EED of the escaping electron, whereas it is the confined electron population that produces high charge state ions and confines them electrostatically. A novel diagnostics method to evaluate the EED of the confined electrons from the EED of the escaping electrons, utilizing pulsed operation of the ion source, and the comparison of the results with particle-in-cell simulations are presented elsewhere in these proceedings.³⁴ The detection method of the escaping electron flux sets a limit for the minimum accessible electron energy. The cold electron temperature can be obtained with OES using the line-ratio method, yielding an estimate of 20–40 eV.¹⁶

C. Ion confinement time (τ)

Ion confinement times have been determined experimentally either inferring them from the escaping ion flux³⁶ or measuring the decay times of ion beam currents with pulsed injection of material, i.e., sputtering^{23,31} or 1+ injection,²³ yielding strikingly different results, i.e., 0.5–2 ms vs 10–100 ms, respectively. The difference can be explained by the fact that the first method probes the confinement of the escaping ion population, whereas the second one must be interpreted as a cumulative confinement time measuring the total residence time of a particle extracted at the charge state q . Two experimental observations made with charge breeder ECRISs support using the latter definition: (i) experiments with a short pulse injection of 1+ ions confirm that the cumulative confinement time of ions is indeed measured in tens of milliseconds³⁷ and (ii) there is a strong correlation between the confinement time deduced from the beam current decay transient and the extracted beam current,²³ which directly supports the validity of the last term of Eq. (8). The latter finding suggests that if the ion confinement time (deduced from the beam current decay transient) is too long, the extracted beam current intensity suffers, i.e., the produced ions cannot be efficiently extracted. These measurements together allow quantifying the expected charge breeding efficiency of the radioactive isotopes with varying half-lives from the efficiency measured for stable isotopes of the same element.³⁷ The comparison of ion confinement times in conventional and charge breeder ECR ion sources yielding similar results²³ implies that the discharge properties are comparable and, thus, supports the use of stable ion beams in the development of sources for radioactive beams where optimizing the ion confinement time is important to first produce the high charge state ions by electron impact ionization and then extract them before a significant loss of ions through radioactive decay. This is further motivated by the similarity of the simultaneously measured charge breeding times and cumulative confinement times.^{23,38}

The long ion confinement time is commensurate with the estimate based on the electron density and ion source performance derived from Fig. 2. Furthermore, it supports the experimentally observed ion temperatures of 5–28 eV derived from the Doppler broadening of ion emission lines.¹⁸ Such high ion temperatures are presumably reached via energy exchange between the ions and the cold electron population as the ions can escape from the electrostatic confinement only if they have sufficient kinetic energy to overcome the $\Delta\Phi$ potential barrier. This qualitative model is convergent with the fact that high charge state ions have the longest confinement times^{23,31} and temperatures.¹⁸ In addition, the electrostatic confinement model is supported by experimental evidence²² showing that the ion-ion collision frequency of high charge state ions exceeds their gyrofrequency, prohibiting magnetic ion confinement. The measured ion temperatures match well with those reported for a quadrupole mirror fusion device³⁹ and predicted theoretically for minimum-B ECRIS⁴⁰ but pose a problem for modeling of ECRIS charge breeders where low T_i of the buffer gas species has to be imposed to match with experimental observations.⁴¹ The above ion temperatures¹⁸ have been measured for discharges with only a single element being injected as neutral gas, whereas recent experiments⁴² with gas mixing show that the temperature of high charge state argon ions can be reduced to 5–8 eV by mixing with oxygen.

Finally, the measurement of the ion confinement times of different charge states helps explain the detrimental effect of kinetic instabilities on the beam currents of high charge state ions.⁵ Since the repetition rate of the periodic instabilities is typically in the range of 0.1–1 kHz, a high charge state ion must survive 1–100 instability events, each of them leading to particle losses on the order of 1%–10% of the total population,⁴³ which translates into less than 10% probability (on average) of reaching high charge states in comparison with the stable regime.

IV. FUTURE DIRECTIONS

Several techniques such as wall coatings,⁴⁴ biased disc,⁴⁵ gas mixing,⁴⁶ frequency tuning,⁴⁷ and multiple frequency heating⁴⁸ increasing the ECRIS performances have been developed over the years. These methods are undoubtedly very useful in improving the charge state distribution of the extracted beams and the stability of the plasma. However, the collective experience gained in operating different generation ECR ion sources still underlines the importance of increasing the magnetic field strength and microwave frequency as a primary direction to push the boundaries of ECRIS capabilities.

For the practical design of the next generation sources, it is not important to decide whether the performance scales with B^2 or f^2 as long as the semiempirical scaling laws [Eqs. (2)–(5)] connecting the two are supported by the experimental evidence. Thus, the design choices of the next generation ECRISs must accommodate magnetic field strengths that are at the limit (or above) of today's superconducting technologies and utilize microwave coupling schemes, e.g., quasioptical structures applied in gasdynamic ion sources,²⁰ allowing us to inject very high microwave powers and frequencies. Alternatively, the concept of the minimum-B field being a superposition of a solenoid and sextupole fields could be revised as pioneered by the SEISM 60 GHz prototype ECRIS⁴⁹ utilizing room-temperature high magnetic field helix-technology to achieve a minimum-B cusp-field or the ARC-ECRIS concept, derived from magnetic confinement fusion experiments and prototyped⁵⁰ at 6.4 GHz. The latter concept has been shown by simulations⁸ to be feasible up to 100 GHz with Nb₃Sn.

Besides delivering beams for users, the 1st–3rd generation sources can be used for testing novel concepts, e.g., different plasma chamber geometries enabling innovative microwave coupling structures¹⁰ and alternative field topologies, as well as for further development of plasma diagnostics studies. Development of such prototypes is often too venturesome to be carried out with the cutting-edge superconducting technologies or in large-scale user facilities inclined to rely on proven technologies, which leaves the field open for smaller laboratories and universities to first demonstrate new technologies and their scalability for high performance sources. Nevertheless, transferring the results obtained with sources operating at frequencies of 14 GHz and below to the next generation ones must be done cautiously. For example, the frequency tuning method⁴⁷ that has been shown to be very effective in improving the coaxial coupling in the 2nd generation sources yields diminishing returns in sources using direct waveguide coupling⁵¹ or a higher plasma chamber dimension to wavelength-ratio.

An example of possible modifications to the plasma chamber geometry of a conventional minimum-B ECRIS and its magnetic

field topology, derived from plasma diagnostics experiments, has been recently reported by Toivanen⁵² discussing experiments using a cylindrical structure around the extraction aperture extruding toward the ECRIS plasma with the “collar” exhibiting very little evidence of interaction with plasma particles up to a length of 30–40 mm. This indicates that the volume around the collar could be occupied with an additional coil modifying the magnetic field strength at the extraction mirror without affecting the field near the resonance zone, which would be an inevitable consequence of changing the current of the main extraction coil. Such a concept is envisioned to improve the extracted beam currents by reducing the plasma confinement only locally, thus directing the distribution of the escaping particle flux toward the extraction and passing through the “extraction channel,” as witnessed in the collar experiment.⁵² Controlling the ion losses is seen as a promising method to improve the performances of ECR ion sources as the existence of the well-known afterglow effect, recent OES experiments,⁵³ and the correlation between the confinement time and the extracted beam current²³ all imply that the extracted currents in cw operation mode could be limited by the electrostatic ion confinement and particle losses rather than the rate of their production by electron impact ionization.

Another, more radical, example of the development of alternative ECRIS concepts is the 10 GHz CUBE-ECRIS project at JYFL. The CUBE-ECRIS is a permanent magnet version of the ARC-ECRIS intended to further demonstrate the feasibility of the quadrupolelike minimum-B magnetic field topology for high charge state ion beam production and study the extraction of high charge state ion beams through a rectangular slit matching the pattern of the escaping ion flux intercepting with the plasma electrode. The concept is depicted in Fig. 3, showing a schematic of the permanent magnet array and the simulated magnetic field along the Cartesian axes passing through the minimum-B. The detailed design and first results of the CUBE-ECRIS will be reported elsewhere. The permanent magnet design carries its own merit and has potential applications in high charge state ion beam production, but most importantly, it paves the way for the development of a

high-frequency ARC-ECRIS being a possible breakthrough in ECRIS technology. The permanent magnet structure allows multiple lines-of-sights into (and through) the discharge which is ideal for combining diagnostics required for simultaneous measurement of electron density (interferometry), electron energy distribution (energy spectrum of escaping electrons and plasma bremsstrahlung emission), and ion confinement time and temperature (pulsed material injection by sputtering and optical emission spectroscopy) as well as the appearance of kinetic instabilities at various plasma heating frequencies.

While there has been significant progress in ECRIS plasma diagnostics in the past decades, there are still several diagnostics needs and experiments that could assist the development of the next generation sources:

- One of the most acute needs is the development of reliable, noninvasive tool to measure the plasma density, which would help determining whether or not the $I_q \propto f^2$ scaling is indeed due to the corresponding increase in the plasma density.
- The main challenge related to the measurement of ECRIS plasma parameters via bremsstrahlung diagnostics is the equivocal connection between the actual EED causing the bremsstrahlung emission and the measured spectrum of plasma and thick-target (wall) bremsstrahlung. Furthermore, the difference between the confined and escaping electron population (EED) remains poorly understood. While the measurement of the bremsstrahlung spectrum undoubtedly helps the development of the next generation sources, for example, by allowing us to estimate the cryostat heat load and required radiation protection, it tells very little about the actual plasma processes eventually leading to the emission. Thus, there is an acute need to develop methods to first connect the bremsstrahlung spectrum to the EED of the escaping electrons and finally to the EED of the confined population at different plasma heating frequencies and magnetic field strengths.

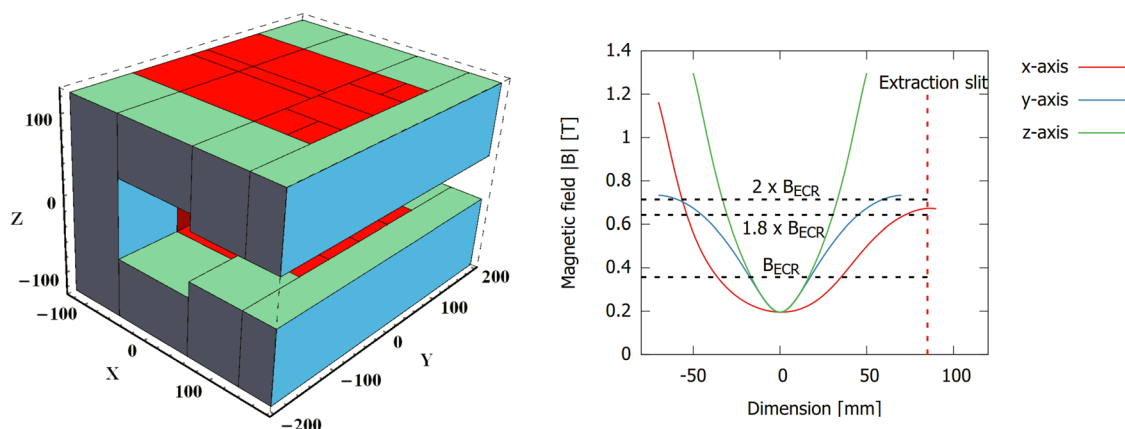


FIG. 3. A schematic drawing of the CUBE-ECRIS permanent magnet array (left). The inner layer itself is suitable for 6.4 GHz operation, whereas the outer layer boosts the field strength enabling to achieve a closed surface of $1.9 \times B_{ECR}$ for 10 GHz. The simulated field strength along the axes passing through the minimum-B is shown on the left. The plasma loss pattern is best suited for a slit extraction located at the yz-plane where $x = 85$ mm.

- From the operational point-of-view, it is crucial to avoid kinetic plasma instabilities and, therefore, develop diagnostics methods that can be used on daily basis by the ion source operators for the detection of the instability threshold when setting up the source to deliver high charge state beams. Such methods include fast measurement of the microwave radiation emitted by the ion source, fast diagnostics of fluctuations in the bremsstrahlung power flux with scintillator detectors, and the adaptation of on-line Fourier analysis of the extracted beam current.⁵⁴ At the fundamental level, it would be necessary to understand which magnetic field parameters, e.g., B_{\min} , B_{\min}/B_{ECR} , $\left(\frac{\vec{B} \cdot \nabla \vec{B}}{|\vec{B}|}\right)_{\text{ECR}}$, are the most influential ones in affecting the high-energy tail of the EED and triggering the instabilities. Fortunately, such experiments are underway in several laboratories (JYFL, LPSC, NSCL-MSU, and IMP). Most importantly, it is necessary to understand how to suppress the instabilities. A well-proven method for this is multiple frequency heating,³⁵ which allows extending the parameter space available for the optimization of the high charge state ion currents and, hence, following the predicted power scaling of $P_{\text{RF}} \propto f_{\text{RF}}^2$ in sources with large plasma chambers. However, the exact mechanism for the instability suppression by multiple frequency heating remains unclear and is actively investigated.^{34,55}
- The experiments probing the ion temperature,¹⁸ the discrepancy between the confined ion population and the extracted beam,⁵³ and ion confinement time^{23,31} support the view that the ions are electrostatically confined and need to acquire a certain energy to overcome the $\Delta\Phi$ potential barrier and become extracted. Such diagnostics methods could now be used for probing the effects of various techniques such as the biased disc, multiple frequency heating, and, perhaps most importantly, gas mixing on the ion temperature and confinement time. Such experiments could be used to determine whether a better control of the ion flux distribution, decoupled from the electron heating (see the discussion on the collar above), could improve the performances of the existing and next generation sources. It is also desirable to measure the ion temperature in a charge breeder ECRIS and compare the results to those obtained with a conventional minimum-B source to support further development of simulation tools developed for the $1+ \rightarrow n+$ technique.⁴¹
- The understanding of the nature of microwave-plasma coupling, i.e., cavity-dominated buildup of EM-fields resulting in strong frequency dependence and spatial distribution of electron heating⁵⁶ vs single-pass absorption, is not well-developed. The large uncertainty in the RF field strengths in ECRIS plasma chambers could be alleviated by further measurements with calibrated RF probes⁵⁷ or the detection of optical emission line shift due to the second-order Stark effect. These measurements would be valuable for computer codes used for simulating the electron heating process in ECRIS plasmas.

The ECRIS plasma diagnostics experiments themselves carry a scientific value. However, for the development of existing and next generation ion sources, the most important question is how do the

plasma properties affect the intensity and quality of the extracted ion beam? This underlines the importance of carrying out all ECRIS plasma diagnostics experiments simultaneously with the analysis of the extracted beam (current and CSD) or under conditions relevant for ion beam production.

ACKNOWLEDGMENTS

This work has received funding from the European Union's Horizon 2020 research and innovation program under Grant Agreement No. 654002, the Academy of Finland under the Finnish Centre of Excellence Program 2012–2017 (Nuclear and Accelerator Based Physics Research at JYFL, Project No. 213503), and the Academy of Finland Project Funding (No. 315855). The research of V. A. Skalyga and I. V. Izotov was carried out within the state assignment of the Ministry of Science and Higher Education of the Russian Federation No. 0035-2019-0002.

REFERENCES

- ¹R. Geller, *Electron Cyclotron Resonance Ion Sources and ECR Plasmas* (Taylor & Francis, 1996).
- ²R. Geller, *Annu. Rev. Nucl. Part. Sci.* **40**, 15 (1990).
- ³D. Hitz, A. Girard, G. Melin, S. Gammino, G. Ciavola, and L. Celona, *Rev. Sci. Instrum.* **73**, 509 (2002).
- ⁴O. Tarvainen *et al.*, *Plasma Sources Sci. Technol.* **23**, 025020 (2014).
- ⁵O. Tarvainen *et al.*, *Rev. Sci. Instrum.* **87**, 02A703 (2016).
- ⁶D. Leitner, C. M. Lyneis, T. Loew, D. S. Todd, S. Virostek, and O. Tarvainen, *Rev. Sci. Instrum.* **77**, 03A302 (2006).
- ⁷C. Lyneis, P. Ferracin, S. Caspi, A. Hodgkinson, and G. L. Sabbi, *Rev. Sci. Instrum.* **83**, 02A301 (2012).
- ⁸P. Suominen and F. Wenander, *Rev. Sci. Instrum.* **79**, 02A305 (2008).
- ⁹L. Celona, CERN Yellow Report CERN-2013-007 (2014), pp. 443–462; e-print arXiv:1411.0546.
- ¹⁰G. Torrisi *et al.*, *J. Instrum.* **14**, C01004 (2019).
- ¹¹C. M. Lyneis, in *MOA001 in Proceedings of ECRIS2016*, Busan, South Korea, 2016, <http://www.jacow.org>.
- ¹²Y. Higurashi, J. Ohnishi, K. Ozeki, and T. Nakagawa, in *MOOBMH02 in Proceedings of ECRIS-2014*, Nizhny Novgorod, Russia, 2014, <http://www.jacow.org>.
- ¹³L. Panitzsch, T. Peleikis, S. Böttcher, M. Stalder, and R. F. Wimmer-Schweiggruber, *Rev. Sci. Instrum.* **84**, 013303 (2013).
- ¹⁴G. Melin, A. G. Drentje, A. Girard, and D. Hitz, *J. Appl. Phys.* **86**(9), 4772 (1999).
- ¹⁵V. P. Pastukhov, *Rev. Plasma Phys.* **13**, 203–259 (1987).
- ¹⁶R. Kronholm, T. Kalvas, H. Koivisto, and O. Tarvainen, *Rev. Sci. Instrum.* **89**, 043506 (2018).
- ¹⁷A. Girard, *Rev. Sci. Instrum.* **63**, 2676 (1992).
- ¹⁸R. Kronholm, T. Kalvas, H. Koivisto, J. Laulainen, M. Marttinen, M. Sakildien, and O. Tarvainen, *Plasma Sources Sci. Technol.* **28**, 075006 (2019).
- ¹⁹D. Mascali *et al.*, *Rev. Sci. Instrum.* **87**, 095109 (2016).
- ²⁰V. Skalyga *et al.*, *Rev. Sci. Instrum.* **87**, 02A716 (2016).
- ²¹D. Hitz, R. Berreby, and M. Druetta, *Phys. Scr.* **T80**, 511–513 (1999).
- ²²O. Tarvainen *et al.*, *Plasma Sources Sci. Technol.* **24**, 035014 (2015).
- ²³M. Marttinen *et al.*, “Estimating ion confinement times from beam current transients in conventional and charge breeder ECRIS,” *Rev. Sci. Instrum.* (these proceedings).
- ²⁴J. Noland, O. Tarvainen, J. Benitez, D. Leitner, C. Lyneis, and J. Verboncoeur, *Plasma Sources Sci. Technol.* **20**, 035022 (2011).
- ²⁵V. Mironov and J. P. M. Beijers, *Phys. Rev. Spec. Top.–Accel. Beams* **12**, 073501 (2009).
- ²⁶J. Noland, J. Y. Benitez, D. Leitner, C. Lyneis, and J. Verboncoeur, *Rev. Sci. Instrum.* **81**, 02A308 (2010).

- ²⁷T. Ropponen, O. Tarvainen, P. Jones, P. Peura, T. Kalvas, P. Suominen, H. Koivisto, and J. Ärje, *Nucl. Instrum. Methods Phys. Res., Sect. A* **600**, 525 (2009).
- ²⁸M. Sakildien, R. Kronholm, O. Tarvainen, T. Kalvas, P. Jones, R. Thomae, and H. Koivisto, *Nucl. Instrum. Methods Phys. Res., Sect. A* **900**, 40–52 (2018).
- ²⁹R. Racz, S. Biri, J. Palinkas, D. Mascali, G. Castro, C. Caliri, F. P. Romano, and S. Gammino, *Rev. Sci. Instrum.* **87**, 02A741 (2016).
- ³⁰J. Benitez, C. Lyneis, L. Phair, D. Todd, and D. Xie, *IEEE Trans. Plasma Sci.* **45**(7), 1746 (2017).
- ³¹D. Neben *et al.*, in *Proceedings of ECRIS2016*, Busan, South Korea, 2016, <http://www.jacow.org>, p. 128.
- ³²M. Guerra, P. Amaro, C. I. Szabo, A. Gumberidze, P. Indelicato, and J. P. Santos, *J. Phys. B: At., Mol. Opt. Phys.* **46**(6), 065701 (2013).
- ³³I. Izotov, O. Tarvainen, V. Skalyga, D. Mansfeld, T. Kalvas, H. Koivisto, and R. Kronholm, *Plasma Sources Sci. Technol.* **27**, 025012 (2018).
- ³⁴I. Izotov *et al.*, “Measurements of the energy distribution of electrons lost from the minimum B-field—The effect of instabilities and two-frequency heating,” *Rev. Sci. Instrum.* (these proceedings).
- ³⁵V. Skalyga *et al.*, *Phys. Plasmas* **22**, 083509 (2015).
- ³⁶G. Douysset, H. Khodja, A. Girard, and J. P. Briand, *Phys. Rev. E* **61**(3), 3015 (2000).
- ³⁷J. Angot, O. Tarvainen, T. Thuillier, M. Baylac, T. Lamy, P. Sole, and J. Jacob, *Phys. Rev. Accel. Beams* **21**, 104801 (2018).
- ³⁸L. Maunoury *et al.*, “Charge breeding at Ganil: Improvements, results and comparison with the other facilities,” *Rev. Sci. Instrum.* (these proceedings).
- ³⁹C. Petty, D. Goodman, D. Smith, and D. Smatlak, *J. Phys., Colloq.* **50**, C1-783–C1-789 (1989).
- ⁴⁰G. D. Shirkov, C. Mühle, G. Musiol, and G. Zschornack, *Nucl. Instrum. Methods Phys. Res., Sect. A* **302**, 1–5 (1991).
- ⁴¹A. Galatà, D. Mascali, L. Neri, and L. Celona, *Plasma Sources Sci. Technol.* **25**, P045007 (2016).
- ⁴²R. Kronholm *et al.*, “ECRIS plasma spectroscopy with a high resolution spectrometer,” *Rev. Sci. Instrum.* (these proceedings).
- ⁴³O. Tarvainen *et al.*, “The biased disc of an electron cyclotron resonance ion source as a probe of instability-induced electron and ion losses,” *Rev. Sci. Instrum.* (these proceedings).
- ⁴⁴C. M. Lyneis, in *Proceedings of the International Conference on ECR Ion Sources and their Applications, East Lansing* (National Superconducting Cyclotron Laboratory, 1987), Report No. MSUCP-47, p. 42.
- ⁴⁵G. Melin *et al.*, in *Proceedings of the 10th International Workshop on ECR Ion Sources, Knoxville* (Oak Ridge National Laboratory, 1990), p. 1, INS Report No. Conf.-9011136.
- ⁴⁶A. G. Drentje, *Nucl. Instrum. Methods Phys. Res., Sect. B* **9**, 526 (1985).
- ⁴⁷L. Celona *et al.*, *Rev. Sci. Instrum.* **79**, 023305 (2008).
- ⁴⁸Z. Q. Xie and C. M. Lyneis, in *Proceedings of the 12th International Workshop on ECR Ion Sources, Riken* (RIKEN Accelerator Laboratory, Japan, 1995), p. 24.
- ⁴⁹T. Lamy *et al.*, in *Proceedings of 13th Heavy Ion Accelerator Technology Conference (HIAT2015)*, Yokohama, Japan, 7–11 September 2015, <http://www.jacow.org>.
- ⁵⁰P. Suominen, T. Ropponen, and H. Koivisto, *Nucl. Instrum. Methods Phys. Res., Sect. A* **578**(2), 370–378 (2007).
- ⁵¹V. Toivanen, H. Koivisto, O. Steczkiewicz, L. Celona, O. Tarvainen, T. Ropponen, S. Gammino, D. Mascali, and G. Ciavola, *Rev. Sci. Instrum.* **82**, 029901 (2011).
- ⁵²V. Toivanen, O. Tarvainen, J. Komppula, and H. Koivisto, *Nucl. Instrum. Methods Phys. Res., Sect. A* **726**, 41–46 (2013).
- ⁵³R. Kronholm, M. Sakildien, D. Neben, H. Koivisto, T. Kalvas, O. Tarvainen, J. Laulainen, and P. Jones, *AIP Conf. Proc.* **2011**, 040014 (2018).
- ⁵⁴V. Toivanen, O. Tarvainen, J. Komppula, and H. Koivisto, *J. Instrum.* **8**, T02005 (2013).
- ⁵⁵E. Naselli *et al.*, *Plasma Sources Sci. Technol.* **28**, 085021 (2019).
- ⁵⁶F. Consoli, L. Celona, G. Ciavola, S. Gammino, F. Maimone, S. Barbarino, R. S. Catalano, and D. Mascali, *Rev. Sci. Instrum.* **79**, 02A308 (2008).
- ⁵⁷V. Toivanen, O. Tarvainen, C. Lyneis, J. Kauppinen, J. Komppula, and H. Koivisto, *Rev. Sci. Instrum.* **83**, 02A306 (2012).